The Adipokine Lipocalin 2 Is Regulated by Obesity and Promotes Insulin Resistance

Qing-Wu Yan,[1] Qin Yang,[1] Nimesh Mody,[1] Timothy E. Graham,[1] Chung-Hsin Hsu,[1] Zhao Xu,[1] Nicholas E. Houstis,[2] Barbara B. Kahn,[1] and Evan D. Rosen[1,2]

OBJECTIVE—We identified lipocalin 2 (*Lcn2*) as a gene induced by dexamethasone and tumor necrosis factor-α in cultured adipocytes. The purpose of this study was to determine how expression of *Lcn2* is regulated in fat cells and to ascertain whether *Lcn2* could be involved in metabolic dysregulation associated with obesity.

RESEARCH DESIGN AND METHODS—We examined *Lcn2* expression in murine tissues and in 3T3-L1 adipocytes in the presence and absence of various stimuli. We used quantitative Western blotting to observe *Lcn2* serum levels in lean and obese mouse models. To assess effects on insulin action, we used retroviral delivery of short hairpin RNA to reduce *Lcn2* levels in 3T3-L1 adipocytes.

RESULTS—*Lcn2* is highly expressed by fat cells in vivo and in vitro. Expression of *Lcn2* is elevated by agents that promote insulin resistance and is reduced by thiazolidinediones. The expression of *Lcn2* is induced during 3T3-L1 adipogenesis in a CCAAT/enhancer-binding protein–dependent manner. *Lcn2* serum levels are elevated in multiple rodent models of obesity, and forced reduction of *Lcn2* in 3T3-L1 adipocytes improves insulin action. Exogenous *Lcn2* promotes insulin resistance in cultured hepatocytes.

CONCLUSIONS—*Lcn2* is an adipokine with potential importance in insulin resistance associated with obesity. ***Diabetes* 56: 2533–2540, 2007**

The worldwide epidemic of obesity and type 2 diabetes has focused attention on adipocyte biology and the role of adipose tissue in the integration of systemic metabolism (1). The discovery of leptin more than a decade ago established a paradigm in which secreted proteins from adipocytes coordinate energy balance and glucose homeostasis (2,3). Since that initial discovery, the number of adipocyte-derived signaling molecules has grown ever larger, and the term adipokine was coined to reflect that many of these molecules exert positive or negative actions on inflammation. Several adipokines promote insulin sensitivity, including leptin (2), adiponectin (4), and visfatin (5), while others induce insulin resistance, such as resistin (6) and retinol binding protein (RBP)4 (7).

Lipocalin 2 (*Lcn2*)—also known as neutrophil gelatinase–associated lipocalin, siderocalin, and 24p3—is a member of a large superfamily of proteins that includes RBP4. Lipocalins are small generally secreted proteins with a hydrophobic ligand binding pocket (8). Known ligands for lipocalins include retinol, steroids, odorants, pheromones, and, in the case of *Lcn2*, siderophores (9). Siderophores are small molecules used by bacteria to poach iron from their hosts, a necessary cofactor for the growth of some pathogens. *Lcn2* is used by the mammalian-innate immune system to sequester siderophore and thus deprive the bacteria of iron. Mice lacking *Lcn2* appear normal but die when exposed to siderophore-requiring strains of bacteria in quantities that are cleared easily by wild-type mice (10,11). *Lcn2* can thus be considered an iron transport protein, and it has been implicated in the apoptotic induction of pro–B-cells (12) and in the biology of the genitourinary system, both as a developmental factor and as a protective mechanism in renal ischemia (13).

In this study, we identify *Lcn2* as a factor dramatically induced by dexamethasone (Dex) and tumor necrosis factor (TNF)-α in 3T3-L1 adipocytes and show that adipose tissue is a dominant site of *Lcn2* expression in the mouse. We also study the regulation of *Lcn2* expression in adipocytes and demonstrate that it is regulated by obesity. We also provide data suggesting that *Lcn2* promotes insulin resistance in adipocytes.

RESEARCH DESIGN AND METHODS

Cell culture and differentiation. 3T3-L1 cells were cultured in Dulbecco's modified Eagle's medium (DMEM) with 10% BCS at 5% CO_2. Once confluence was reached, cells were exposed to DMEM with 10% fetal bovine serum (FBS) containing a prodifferentiative cocktail including Dex (1 μmol/l), insulin (5 μg/ml), and isobutylmethylxanthine (0.5 mmol/l). After 2 days, cells were maintained in medium containing insulin until ready for harvest at day 7. NIH-3T3 cells were maintained in the same conditions. In some experiments, 3T3-L1 cells were differentiated only with 5 μmol/l rosiglitazone plus 10% FBS, which was changed every 2 days. H4IIE rat hepatoma cells were cultured in αMEM medium (Invitrogen), supplemented with 10% FBS at 37°C with 5% CO_2. Cells were seeded in 24-well plates with 50% confluence. Before treatment, cells were washed twice with αMEM containing 0.2% FBS and cultured overnight (18 h) in medium supplemented with or without recombinant *Lcn2* (10 nmol/l)—with Dex treatment (250 nmol/l) in parallel as a positive control. The next day, cells were treated with 100 nmol/l insulin for 30 min, then washed twice with Krebs-Ringer HEPES buffer plus lactate and pyruvate (10 mmol/l HEPES, pH 7.4, 96 mmol/l NaCl, 4.7 mmol/l KCl, 1.25 mmol/l $CaCl_2$, 1.2 mmol/l $MgSO_4$, 1.2 mmol/l KH_2PO_4, 25 mmol/l $NaHCO_3$, 20 mmol/l lactate, and 2 mmol/l pyruvate). Cells were incubated in Krebs-Ringer HEPES buffer and supplemented with *Lcn2*, Dex, or carrier solution for another 6 h at 37°C. Supernatants were collected for the glucose oxidase assay, and cells were harvested by Trizol (Invitrogen) for RNA analysis.

From the [1]Division of Endocrinology, Diabetes, and Metabolism, Beth Israel Deaconess Medical Center, Boston, Massachusetts; and the [2]Broad Institute of Harvard and Massachusetts Institute of Technology, Cambridge, Massachusetts.

Address correspondence and reprint requests to Evan D. Rosen, MD, PhD, Division of Endocrinology, Diabetes, and Metabolism, Beth Israel Deaconess Medical Center, Boston, MA 02115. E-mail: erosen@bidmc.harvard.edu.

Received for publication 3 January 2007 and accepted in revised form 10 July 2007.

Published ahead of print at http://diabetes.diabetesjournals.org on 16 July 2007. DOI: 10.2337/db07-0007.

E.D.R. is listed as an inventor on a patent application related to Lcn2.

C/EBP, CCAAT/enhancer-binding protein; Dex, dexamethasone; DMEM, Dulbecco's modified Eagle's medium; FBS, fetal bovine serum; PPAR, peroxisome proliferator–activated receptor; RBP, retinol binding protein; shRNA, short hairpin RNA; SVC, stromal vascular cell; SVF, stromal vascular factor; TNF, tumor necrosis factor; WAT, white adipose tissue.

Recombinant *Lcn2* was produced as described (13). Endotoxin was assayed in 100 μl of 1 nmol/l recombinant *Lcn2* solution by means of a limulus amoebocyte lysate gel clot assay (0.125 EU/ml sensitivity; Cambrex/Lonza, Allendale, NJ) and was found to be below the limits of detection for the assay.

Animals. All animal studies were conducted in accordance with the principles and procedures outlined in the National Institutes of Health *Guide for the Care and Use of Laboratory Animals*. For the high-fat diet studies, 3- to 4-week-old FVB male mice were obtained from Taconic. Mice were fed a standard chow diet (Formulab 5008) or high-fat diet (55% fat calories; Harlan-Teklad 93075). Animals were put on diet treatment at 4–5 weeks of age, and plasma *Lcn2* levels were measured after 12 weeks (ad libitum–fed state). Nine-week-old *db/db* females and lean littermate controls (+/+ or *db*/+) were obtained from Charles River (n = 8 each). Mice were fed a standard chow diet (Formulab 5008), and plasma *Lcn2* levels were measured in the ad libitum–fed state. Male *ob/ob* or *ob*/+ mice were purchased from The Jackson Laboratories (Bar Harbor, ME) and studied at 10 months of age.

Northern blotting. Cells were lysed in Trizol and processed according to the manufacturer's instructions. Murine tissues were harvested from wild-type C57BL/6J mice. For each sample, 10 μg total RNA was loaded onto formaldehyde-agarose gels, transferred onto nylon membranes, and hybridized with the appropriate ^{32}P-labeled probe in Ultrahyb (Ambion).

Quantitative PCR. First-strand cDNA synthesis for quantitative PCR was performed using RETROscript (Ambion). Total RNA (1.5 mg) was converted into first-strand cDNA using oligo dT primers as described in the kit. cDNA was amplified and detected with the Brilliant SYBR Green QPCR master mix (Stratagene) according to the manufacturer's instruction. Real-time PCR was performed in an Mx3000P thermocycler (Stratagene), and its software was used to calculate the cycle threshold of each reaction. Validation experiments were performed to demonstrate equal efficiencies of target *Lcn2* and of internal control (18S rRNA for tissues and cyclophilin for 3T3-L1 cells). The relative amount of *Lcn2* transcripts was determined using comparative C_t method with the expression level of untreated control as 1. Primer sequences are as follows: m18S-F, AGTCCCTGCCCTTTGTACACA; m18S-R, GATCCGAGG GCCTCACTAAAC; mCyclophilin-F, GGTGGAGAGCACCAAGACAG; mCyclophilin-R, GCCGGAAGTCGACAATGATG; mLcn2-F, ACTTCCGGAGCGATCAG TT; mLcn2-R, CAGCTCCTTGGTTCTTCCAT; mFabp4-F, TGGAAGCTTGTCTC CAGTGA; mFabp4-R, CTTGTGGAAGTCACGCCTTT; mPparg-F, GCATGGT GCCTTCGCTGA; mPparg-R, TGGCATCTCTGTGTCAACCATG; mLeptin-F, AGAAGATCCCAGGGAGGAAA; mLeptin-R, TCATTGGCTATCTGCAGCAC; mGlut1-F, TTGGAGAGAGAGCGTCCAAT; mGlut1-R, CTCAAAGAAGGCCA CAAAGC; rG6Pase-F, ACCCTGGTAGCCCTGTCTTT; rG6Pase-R, ACTCATTA CACGGGCTGGTC.

Plasma *Lcn2* measurement. Plasma (1 μl) was diluted 30 times in 1× Laemmli buffer; proteins were separated by SDS-PAGE on 15% gels and transferred to nitrocellulose membranes. A single band for Lcn2 protein was detected at ~23 kDa using anti-mouse lipocalin-2–specific goat IgG (catalog no. AF1857; R&D Systems). Bands were quantitated by densitometry, with three control samples on each membrane providing standardization between membranes. Concentrations are arbitrary units per microliter of plasma, with controls set at 1.

Isolation of adipocytes, macrophages, and nonmacrophage stromal vascular cells from perigonadal adipose tissue. Five-week-old male C57BL/6J mice were obtained from The Jackson Laboratories and were fed chow or high-fat diets (Research Diets D12331) beginning at 6 weeks of age (n = 7 each group). At 26–34 weeks of age, fed mice were killed by CO_2 inhalation and epididymal adipose tissue (~0.5 g) collected and placed in Krebs-Ringer HEPES buffer containing 10 mg/ml fatty acid–poor BSA (Sigma-Aldrich, St. Louis, MO). The tissue was minced into fine pieces and centrifuged at 1,000*g* for 10 min to remove erythrocytes and other blood cells. Minced tissue was then digested in 0.12 units/ml of low-endotoxin collagenase (Liberase 3; Roche Applied Science, Indianapolis, IN) at 37°C in a shaking water bath (80 Hz) for 45 min. Samples were then filtered through a sterile 300-μm nylon mesh (Spectrum Laboratories, Rancho Dominguez, CA) to remove undigested fragments. The resulting suspension was centrifuged at 500*g* for 10 min to separate stromal vascular cells (SVCs) from adipocytes. Adipocytes were removed and washed with Krebs-Ringer HEPES buffer, then suspended in Trizol for RNA isolation. The SVC fraction was incubated in erythrocyte lysis buffer (0.154 mmol/l NH_4Cl, 10 mmol/l $KHCO_3$, and 0.1 mmol/l EDTA) for 2 min. Cells were then centrifuged at 500*g* for 5 min and resuspended in 100 μl fluorescence-activated cell sorter buffer (PBS containing 5 mmol/l EDTA and 0.2% fatty acid–poor BSA). The cells were incubated in the dark on a bidirectional shaker with FcBlock (20 μg/ml; BD Pharmingen, San Jose, CA) for 30 min at 4°C. They were then incubated for 50 min with APC-conjugated primary antibody against F4/80 (5 μg/ml; Caltag Laboratories, Burlingame, CA) and phycoethrin-conjugated antibody against CD11b (2 μg/ml Mac-1). Control aliquots of SVCs were incubated with APC-labeled (2 μg/ml) and phycoethrin-labeled (5 μg/ml) isotype control antibodies (Caltag Laboratories). After incubation, cells were washed and suspended in fluorescence-activated cell sorter buffer. F4/80+/CD11b+ macrophages and F4/80−/CD11b− nonmacrophage SVCs were isolated with a MoFlo (DakoCytomation, Fort Collins, CO) fluorescence-activated flow sorter. After sorting, F4/80+/CD11b+ and F4/80−/CD11b− cells were suspended in Trizol for RNA isolation.

Retroviral infections. Retroviruses were constructed in pMSCV (Clontech) using either puromycin- or hygromycin-selectable markers. Viral constructs were transfected into 293T cells using CellPhect transfection kits (GE Healthcare) along with plasmids expressing gag-pol and the VSV-G protein. Supernatants were collected after 48 h. After filtration to remove cell debris, supernatants were added to either 3T3-L1 or NIH-3T3 cells at 70% confluence; selection with puromycin (4 μg/ml) or hygromycin (175 μg/ml) was started 48 h later. Cells were selected and studied immediately or frozen for later use.

Promoter constructs, cotransfection, and luciferase assay. Oligonucleotides were selected to amplify fragments of 1,742, 731, 320, 222, and 131 bp specific to the 5′-untranslated region of the murine *Lcn2* promoter and to include restriction enzyme cutting sites for facilitating cloning into the pA3-luc reporter vector. All constructs were confirmed by sequencing. The mutated −222 plasmids were constructed using the same procedure, except the forward primer contained the desired mutation.

NIH-3T3 cells were cotransfected by lipofectamine with the ratio of reporter:β-gal:C/EBP (CCAAT/enhancer-binding protein) expression plasmid as 1:0.1:2. Cells were incubated for 48 h, lysed, and assayed using the Luciferase Reporter Gene Assay kit (Roche). Luciferase activity was normalized to β-gal activity.

Chromatin immunoprecipitation assay. 3T3-L1 cells were treated with 1% formaldehyde for 15 min at room temperature to cross-link DNA with DNA binding protein complexes. The chromatin immunoprecipitation assay was performed using a kit from Upstate. Immunoprecipitation was carried out using 2 μg of the following antibodies: C/EBPα (sc-61), C/EBPβ (sc-150), and C/EBPδ (sc-636) from Santa Cruz Biotechnology. An aliquot of chromatin DNA prepared from the cells taken before immunoprecipitation was used as input DNA. Immunoprecipitated and input DNAs were assayed by PCR with primer pair 5′-CTGCTGACCCACAAGCAGT-3′ and 5′-GGCAAGATTTCTGTCCCT CTC-3′ in the *Lcn2* gene promoter region. Amplified PCR products were visualized on 2% agarose electrophoresis gels.

Short hairpin RNA–mediated *Lcn2* knockdown. Four independent hairpins targeted to murine *Lcn2* were developed using software from Clontech. These hairpins were synthesized and cloned into a retroviral delivery vector (pSIREN-RetroQ; Clontech) and transfected into Phoenix cells. Viral supernatants were used to transduce 3T3-L1 preadipocytes as described (14), and infected cells were selected by 4 μg/ml puromycin 48 h postinfection. Inhibition of *Lcn2* expression was measured by quantitative PCR as well as by Western blotting.

Glucose oxidase assay. For the glucose oxidase colorimetric method, we used the Amplex Red glucose/glucose oxidase assay kit, following the manufacturer's instruction. Absorption at 571 nm was measured in a PowerWave XS microplate spectrophotometer (BioTek). This experiment was performed in triplicate (three wells for each condition).

Glucose uptake assay. 3T3-L1 cells were differentiated as above noted, except that cells were exposed to differentiation regimen (Dex/methylisobutylxanthine/insulin) for 3 days. At day 3, cells were fed with DMEM containing 2% FBS. Fresh media were changed 24 h before the assay. Before the assay, cells were starved for 3 h in serum-free DMEM. Glucose uptake was determined as previously reported (15).

Statistical analysis. Statistics were generally performed with the t test, except for comparisons of serum *Lcn2* levels between lean and obese mice, for which the nonparametric Mann-Whitney test was used because of nonnormal distribution of data or small n.

RESULTS

***Lcn2* expression in 3T3-L1 adipocytes is induced by Dex and TNF-α.** We performed a genomic screen to identify common mechanisms of insulin resistance, using Dex and TNF treatment of 3T3-L1 adipocytes as a model system. The major outcome of this study was the observation that genes associated with reactive oxygen species were affected concordantly by these two highly disparate treatments (14). *Lcn2* was another gene induced strongly by both TNF and Dex in the microarray experiment. This effect was confirmed by quantitative PCR, which showed induction of *Lcn2* mRNA of ~80-fold by Dex and 30-fold by TNF (Fig. 1*A*). The effect of TNF was also seen

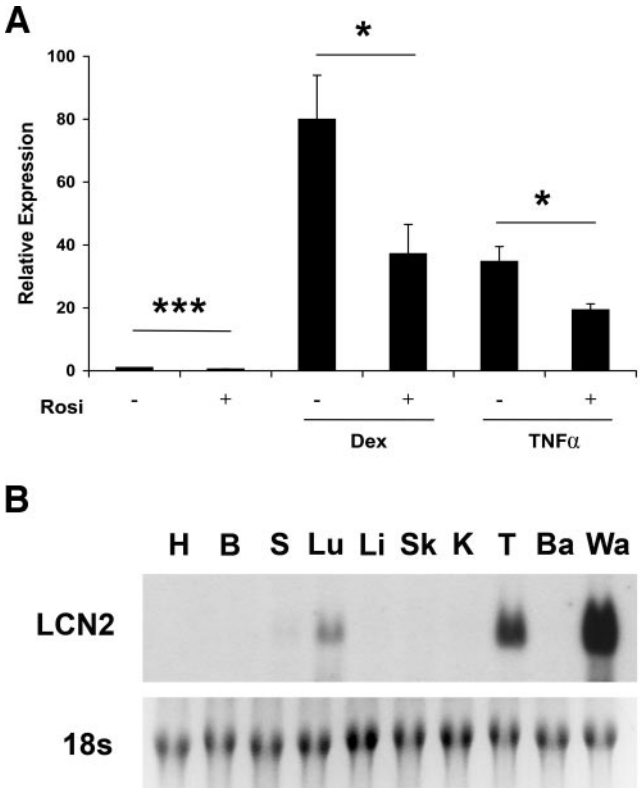

FIG. 1. *Lcn2* is expressed in adipocytes and is regulated by Dex and TNF. *A*: Mature 3T3-L1 adipocytes were treated with Dex (1 μmol/l) or TNF (4 ng/μl) in the presence or absence of rosiglitazone (Rosi) (1 μmol/l), and *Lcn2* mRNA levels were measured by quantitative PCR. Data are means ± SD. *$P < 0.05$, ***$P = 0.005$ relative to no rosiglitazone, $n = 3$. *B*: Northern analysis of murine heart (H), brain (B), spleen (S), lung (Lu), liver (Li), skeletal muscle (Sk), kidney (K), testis (T), brown adipose tissue (Ba), and perigonadal white adipose tissue (Wa) from male C57BL/6 mice.

previously (16). The insulin-sensitizing agent rosiglitazone significantly attenuated *Lcn2* mRNA expression by either agent.

***Lcn2* is highly expressed in adipocytes in vitro and in vivo.** Others have reported *Lcn2* expression in fat (16–19), but there has been no attempt to compare adipose expression to other sites. Northern analysis showed that white adipose tissue (WAT) was by far the dominant site of expression of *Lcn2* in wild-type male mice (Fig. 1*B*). We also saw significant amounts of *Lcn2* mRNA in lung and in testis/epididymis—both reported as major sites of expression (20). We next sought to determine whether *Lcn2* expression is regulated during adipogenesis. 3T3-L1 preadipocytes were differentiated using a standard cocktail containing Dex, methylisobutylxanthine, and insulin, and *Lcn2* expression was assessed with quantitative PCR at various time points. We noted an immediate and profound induction of *Lcn2* mRNA within the first day of differentiation (Fig. 2*A*); levels remained elevated for at least 7 days. The C_t for *Lcn2* in mature 3T3-L1 adipocytes ranges from 21 to 23; the corresponding value in murine WAT is 18. We looked at the contribution of each component of the induction cocktail (Fig. 2*B*) and found that Dex was the dominant contributor to *Lcn2* induction, as expected. However, methylisobutylxanthine also had a significant effect on *Lcn2* levels, and the combination of Dex and methylisobutylxanthine was maximally potent, with no significant contribution from insulin. We were interested to know whether *Lcn2* expression in 3T3-L1 cells was

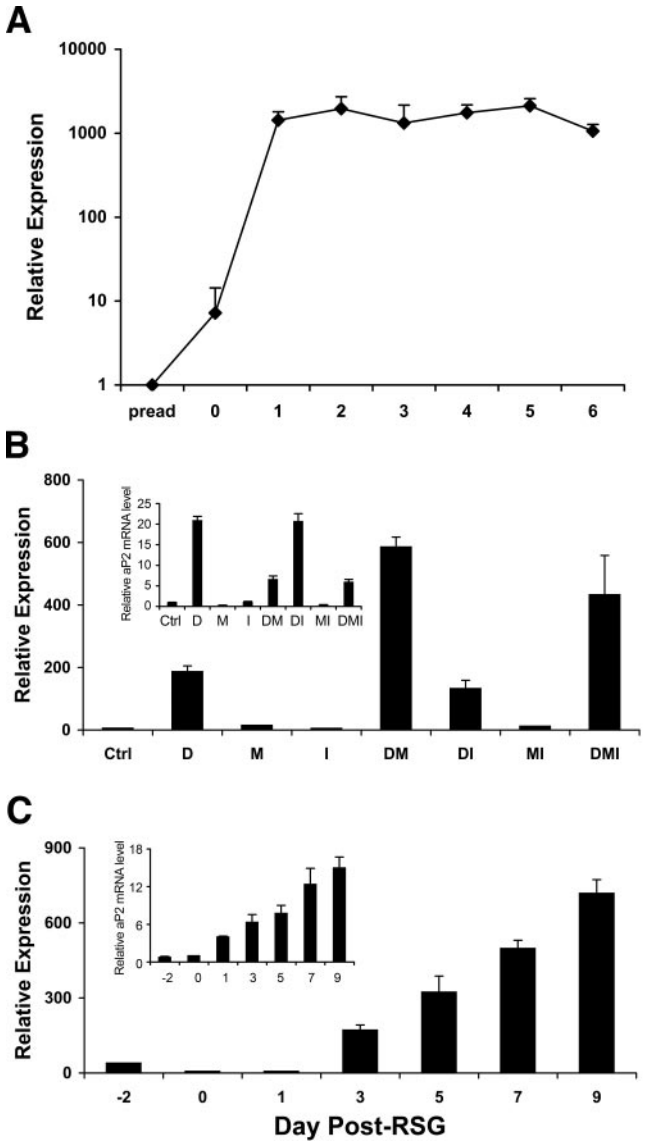

FIG. 2. Expression of *Lcn2* during 3T3-L1 adipogenesis. *A*: Time course of *Lcn2* mRNA expression during 3T3-L1 adipogenesis. Data are means ± SD, $n = 3$. *B*: *Lcn2* mRNA expression in confluent 3T3-L1 preadipocytes treated with Dex (D), methylisobutylxanthine (M), insulin (I), or combinations thereof. Data are means ± SD, $n = 3$. *C*: *Lcn2* expression during 3T3-L1 differentiation induced by rosiglitazone in the absence of Dex/methylisobutylxanthine/insulin (DMI). Data are means ± SD, $n = 3$. For *B* and *C*, the *inset* shows the corresponding amount of *Fabp4* mRNA to mark the extent of differentiation.

dependent on the specific induction cocktail or whether it was linked to adipogenesis per se. This was addressed by differentiating 3T3-L1 cells in the absence of Dex, methylisobutylxanthine, or insulin, using rosiglitazone only. *Lcn2* expression rose more gradually than when Dex/methylisobutylxanthine were present (Fig. 2*C*) but reached similar levels later during differentiation. The apparent contradiction between the effect of rosiglitazone in Figs. 1 and 2 is resolved by considering the developmental status of the cells; in undifferentiated cells, rosiglitazone promotes adipogenesis and thus indirectly promotes *Lcn2* expression. In mature cells, however, the direct effect of rosiglitazone is suppression of *Lcn2* expression.

Expression of *Lcn2* in adipocytes is C/EBP dependent. Many adipocyte genes are transcriptionally regulated by peroxisome proliferator–activated receptor

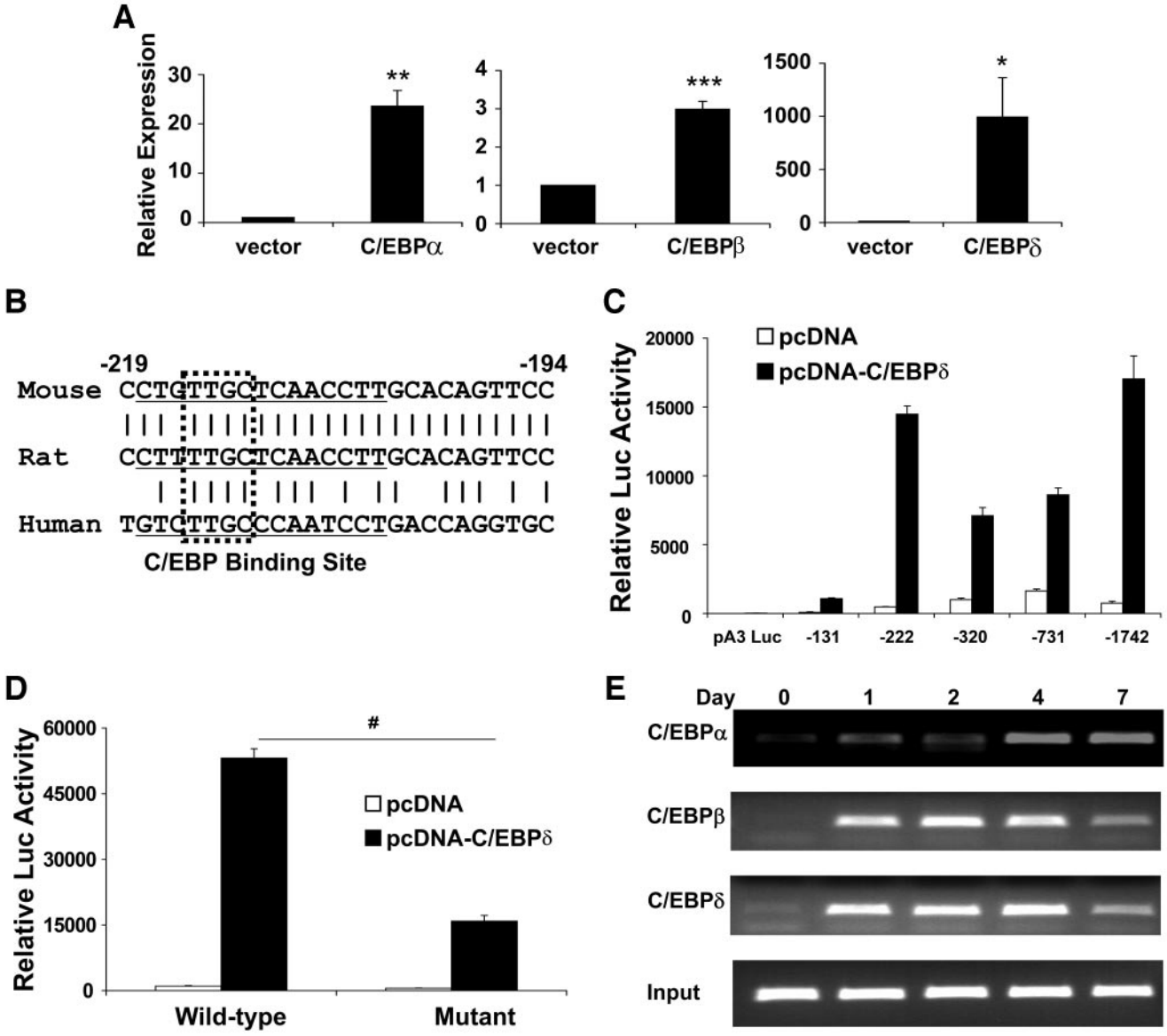

FIG. 3. *Lcn2* expression in adipocytes is C/EBP dependent. *A*: PPARγ$^{-/-}$ cells were infected with C/EBP-expressing retroviruses, and endogenous levels of *Lcn2* were measured by quantitative PCR relative to cells transduced with empty vector. Data are means ± SD. *$P < 0.05$, **$P < 0.01$, ***$P < 0.001$, $n = 3$. *B*: Alignment of mouse, rat, and human *Lcn2* promoter sequences reveals a putative C/EBP binding site. Boxed letters, core nucleotides essential for C/EBP binding. *C*: Deletion analysis of murine *Lcn2* promoter fragments in transiently transfected NIH-3T3 cells in the presence (■) or absence (□) of cotransfected C/EBPδ. Data are means ± SD, $n = 3$. *D*: Mutation analysis of the core C/EBP-binding motif. NIH-3T3 cells were transfected with the wild-type −222 fragment luciferase construct or with the same fragment after mutation of the core TTGC in the presence (■) or absence (□) of cotransfected C/EBPδ. Data are means ± SD, $n = 6$. #$P = 3.3^{-10}$. *E*: Chromatin immunoprecipitation assay of the proximal *Lcn2* promoter in 3T3-L1 cells at different time points after differentiation.

(PPAR)γ and/or members of the C/EBP family of bZIP proteins (18). The ability of rosiglitazone to repress *Lcn2* (Fig. 1*A*) suggested that PPARγ was unlikely to be a direct inducer of *Lcn2* expression. We thus tested whether C/EBP isoforms might serve this purpose. C/EBPα, -β, and -δ, delivered by retroviral transduction, were all effective at inducing endogenous *Lcn2* expression in PPARγ$^{-/-}$ fibroblasts (Fig. 3*A*). These cells were chosen to avoid the confounding effects of simultaneous adipogenesis; C/EBPs cannot induce differentiation in the absence of PPARγ (14). To identify C/EBP binding sites in the *Lcn2* promoter, we performed a computational search (Fig. 3*B*). This revealed a possible C/EBP site with a high degree of conservation between mouse, rat, and humans at −218 of the murine promoter. *Trans*-activation assays in NIH-3T3 cells showed that the ability of C/EBPδ to induce expression of this construct dropped off sharply when deletions were made that eliminated this site (Fig. 3*C*). The same effect was seen with C/EBPα and -β (data not shown). Mutation of the core sequence of this site from TTGC to GGGA significantly decreased the ability of C/EBPδ to *trans*-activate the reporter (Fig. 3*D*). Finally, we used Chromatin Immunoprecipitation to demonstrate specific C/EBP isoform binding to this element in living cells (Fig. 3*E*). Before differentiation, no C/EBP isoform was bound to the site, but C/EBPβ and -δ were highly bound by the first day after induction. By day 4, C/EBPα binds the site as well, which is consistent with the delayed appearance of this factor during 3T3-L1 adipogenesis (21), followed by a reduction in C/EBPβ and -δ binding, which reflects their diminished expression.

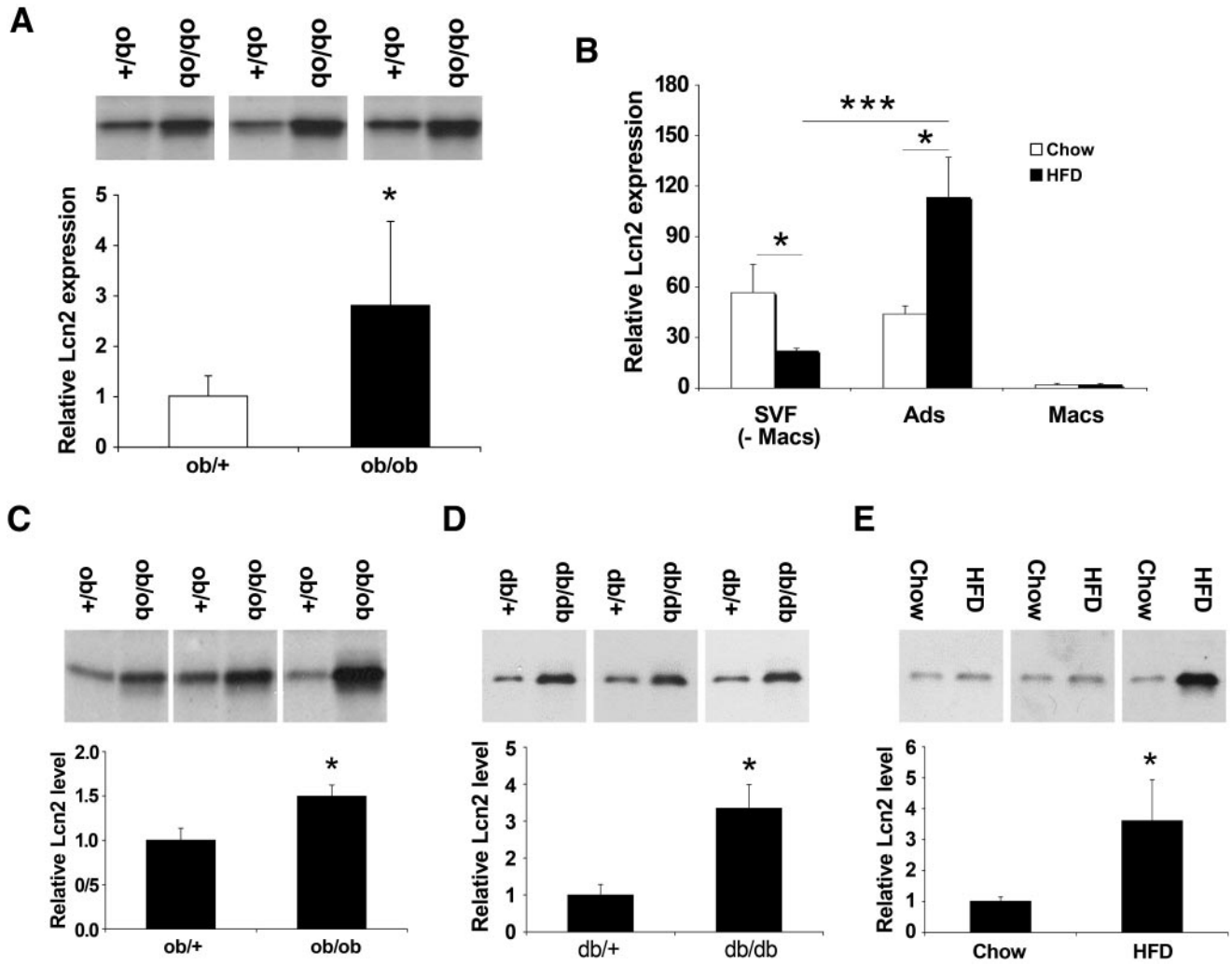

FIG. 4. ***Lcn2*** **is elevated in obesity.** ***A*****: *Lcn2* protein levels in perigonadal WAT lysates (30 μg/lane) from male *ob/+* ($n = 5$) and *ob/ob* ($n = 7$) mice. Data are means ± SD. *$P < 0.05$. *B*: *Lcn2* mRNA expression in fractionated WAT from male C57BL mice given chow ($n = 7$) or high-fat ($n = 7$) diet, relative to expression in chow macrophages. Ads, adipocytes; Macs, macrophages. Data are means ± SD. *$P < 0.05$, ***$P < 0.001$. *C*: *Lcn2* protein levels in serum from fed male *ob/+* ($n = 6$) and *ob/ob* ($n = 10$) mice, measured by Western blotting and expressed as fold relative to the mean of *ob/+* controls. *D*: *Lcn2* protein expression in serum from fed female *db/+* ($n = 8$) and *db/db* ($n = 8$) mice, expressed as fold relative to the mean of *db/+* controls. *E*: *Lcn2* protein expression in serum from chow ($n = 15$) and high-fat–fed male ($n = 18$) mice, expressed as fold relative to the mean of chow-fed controls. Data for *C*, *D*, and *E* are shown as the mean for each group, with representative Western blots from three lean and three obese animals shown on *top*. For SD and statistical analysis, see text.**

Lcn2 **levels are elevated in obesity.** We next looked at whether *Lcn2* expression is altered by obesity. Western blotting of lysates from the adipose tissue of obese (*ob/ob*) mice revealed a significant elevation of *Lcn2* relative to lean controls (Fig. 4*A*). We also examined adipose tissue from mice fed either a chow or high-fat diet after fractionation into mature adipocytes, SVCs, and macrophages (Fig. 4*B*). Lean animals (30.3 ± 0.4 g; $n = 9$) had equivalent *Lcn2* mRNA expression in the adipocyte and SVC fractions, while obese animals (53.0 ± 01.0 g; $n = 8$) shifted *Lcn2* mRNA expression away from the SVC fraction and toward mature adipocytes. There was no significant expression of *Lcn2* in adipose tissue–resident macrophages in either the lean or obese state. We were somewhat surprised to find significant *Lcn2* expression in the stromal vascular fraction (SVF) of lean animals, given the low levels seen in cultured preadipocytes. There are two plausible explanations for this. First, the low-speed centrifugation method used to separate adipocytes from SVF may not separate cells that are early in the differentiation process (i.e., before significant lipid accumulation). Since *Lcn2* appears to be induced early in differentiation, this could account for a higher-than-expected amount of *Lcn2* in the SVF. Alternatively, there may be significant *Lcn2* expression in other cell types in the SVF (e.g., endothelial cells or fibroblasts). Consonant with the data from *ob/ob* mice, Lcn2 protein expression was elevated in WAT of high-fat–fed animals (data not shown). Given the elevated expression in adipose tissue, we next assessed whether increased serum levels of *Lcn2* are associated with excess adiposity. In fact, we found elevated serum *Lcn2* levels in three different murine obesity models. *Lcn2* was increased relative to lean controls in *ob/ob* mice (1.5 ± 0.40-fold, $P = 0.02$) (Fig. 4*C*), *db/db* mice (3.3 ± 1.80-fold, $P = 0.01$) (Fig. 4*D*), and in high-fat feeding (3.6 ± 5.6-fold, $P = 0.03$) (Fig. 4*E*). All of these samples were collected in the fed state to reduce confounding due to possible nutritional influences on *Lcn2* levels. Nonetheless, *Lcn2* levels are still elevated in obese *db/db* mice even in the fasted state (13.6 ± 4.2-fold, $P = 0.01$). The body weights of these mice were as follows: 31.6 ± 0.8 g (chow) vs. 39.9 ± 0.7 g (high-fat diet),

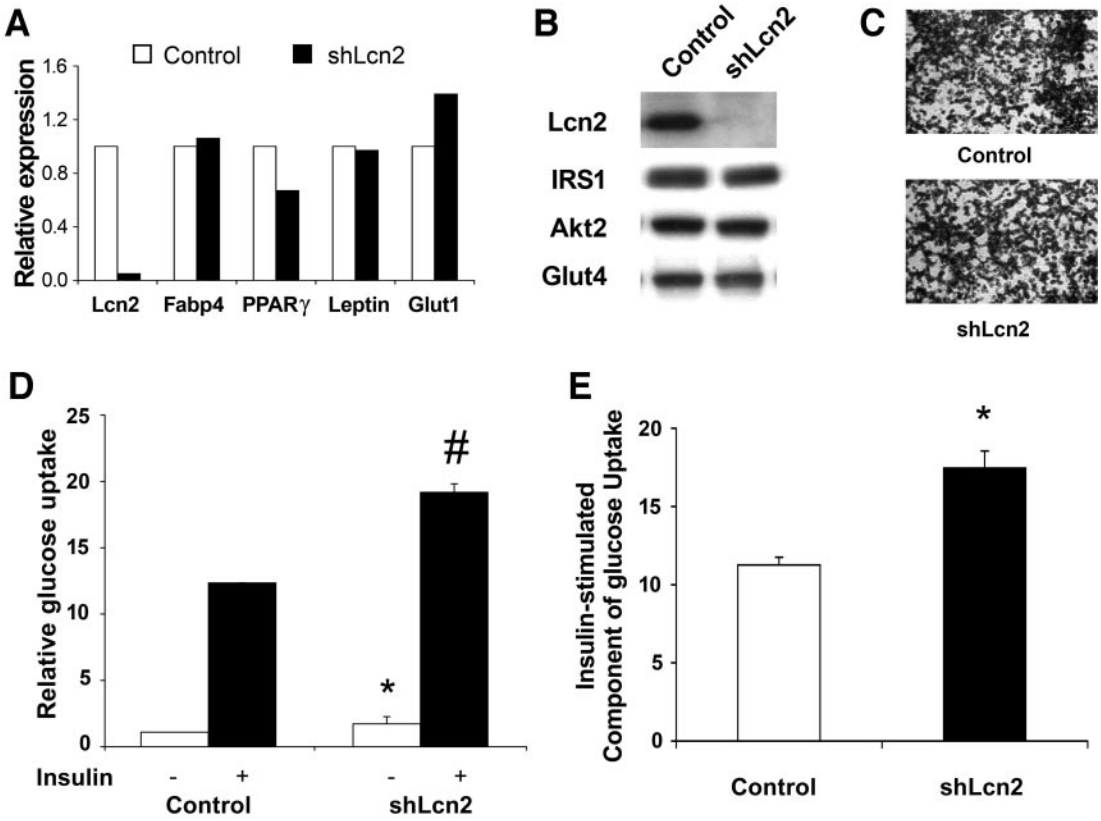

FIG. 5. shRNA-mediated knockdown of *Lcn2* improves insulin action in cultured adipocytes. *A*: mRNA expression of *Lcn2* and markers in mature 3T3-L1 adipocytes expressing either control shRNA or shLcn2. *B*: Protein expression of *Lcn2* and other markers in mature 3T3-L1 adipocytes expressing either control shRNA or shLcn2. *C*: Oil red O staining of mature 3T3-L1 adipocytes expressing either control shRNA or shLcn2. *D*: Basal (□) and insulin-stimulated (■) glucose uptake in mature 3T3-L1 adipocytes expressing either control shRNA or shLcn2. Data are means ± SD, $n = 12$, *$P < 1e^{-5}$ relative to control shRNA, no insulin; #$P = 5e^{-5}$ relative to control shRNA, plus insulin. *E*: Component of glucose uptake attributable to insulin, equivalent to the uptake in the presence of insulin minus the uptake in the absence of insulin. Data are means ± SD, $n = 12$, * $P < 1e^{-4}$.

21.0 ± 0.45 g (*db/+*) vs. 41.3 ± 0.85 g (*db/db*), and 26.0 ± 0.51 g (*ob/+*) vs. 47.7 ± 3.51 g (*ob/ob*).

Lcn2 promotes insulin resistance in cultured adipocytes and hepatocytes. Several factors converge to suggest that Lcn2 may promote insulin resistance, including serum elevation in obesity, induction by TNF and Dex, repression by thiazolidinediones, and structural similarity to RBP4. We attempted to test this directly by adding purified Lcn2 to mature 3T3-L1 adipocytes and then measuring insulin-stimulated glucose uptake, but we were unable to find a consistent change in glucose uptake in the presence of Lcn2, either as apo-Lcn2 or after the protein was incubated with a siderophore-iron complex (data not shown). We were concerned that this might reflect that Lcn2 is not limiting in the culture medium of 3T3-L1 adipocytes, which produce and secrete large amounts of the protein. The amount of Lcn2 in conditioned medium is similar to that seen in the serum of obese mice (data not shown). We thus approached this issue from a different direction by asking whether reducing Lcn2 levels lead to improved insulin action. This was accomplished through retroviral delivery of short hairpin (sh)RNA directed against Lcn2. We identified a hairpin that reduced expression of Lcn2 by >90%, as measured by quantitative PCR (Fig. 5*A*) or Western blot (Fig. 5*B*). Importantly, cells expressing this shRNA were differentiated to the same degree as cells expressing a control hairpin, as determined by oil red O staining of lipid accumulation (Fig. 5*C*) and marker expression (Fig. 5*A* and *B*). Cells expressing the Lcn2 shRNA, however, showed elevated glucose uptake in both the basal and insulin-stimulated states (Fig. 5*D*). Importantly, the component of glucose uptake that reflects insulin action (i.e., the difference between the insulin-stimulated and the basal glucose uptake) was significantly elevated in cells expressing the Lcn2 shRNA (Fig. 5*E*).

We next tested whether exogenous Lcn2 could affect insulin sensitivity in cultured H4IIe hepatocytes. In the absence of insulin, Lcn2 did not affect glucose production (Fig. 6*A*) or glucose 6-phosphatase expression (Fig. 6*B* and *C*). Lcn2 did, however, partially block the suppressive effects of insulin on these parameters. No effect of Lcn2 was seen on PEPCK mRNA levels, either in the presence or absence of insulin (data not shown). Importantly, the magnitude of insulin resistance induced by Lcn2 in these cells was comparable to that achieved with Dex. Interestingly, apo-Lcn2 (i.e., not complexed with siderophore and iron) was unable to induce insulin resistance in cultured hepatocytes (Fig. 6*D*).

DISCUSSION

It is now appreciated that adipocytes secrete a wide array of proteins that influence systemic metabolism. These include factors that promote insulin sensitivity as well as others that induce insulin resistance (3). We show here that Lcn2 is highly expressed in adipocytes, that its expression is regulated by obesity, and that it induces insulin resistance. In this sense, it behaves in a very similar fashion to RBP4, another member of the lipocalin superfamily and a close relative of Lcn2. While others have

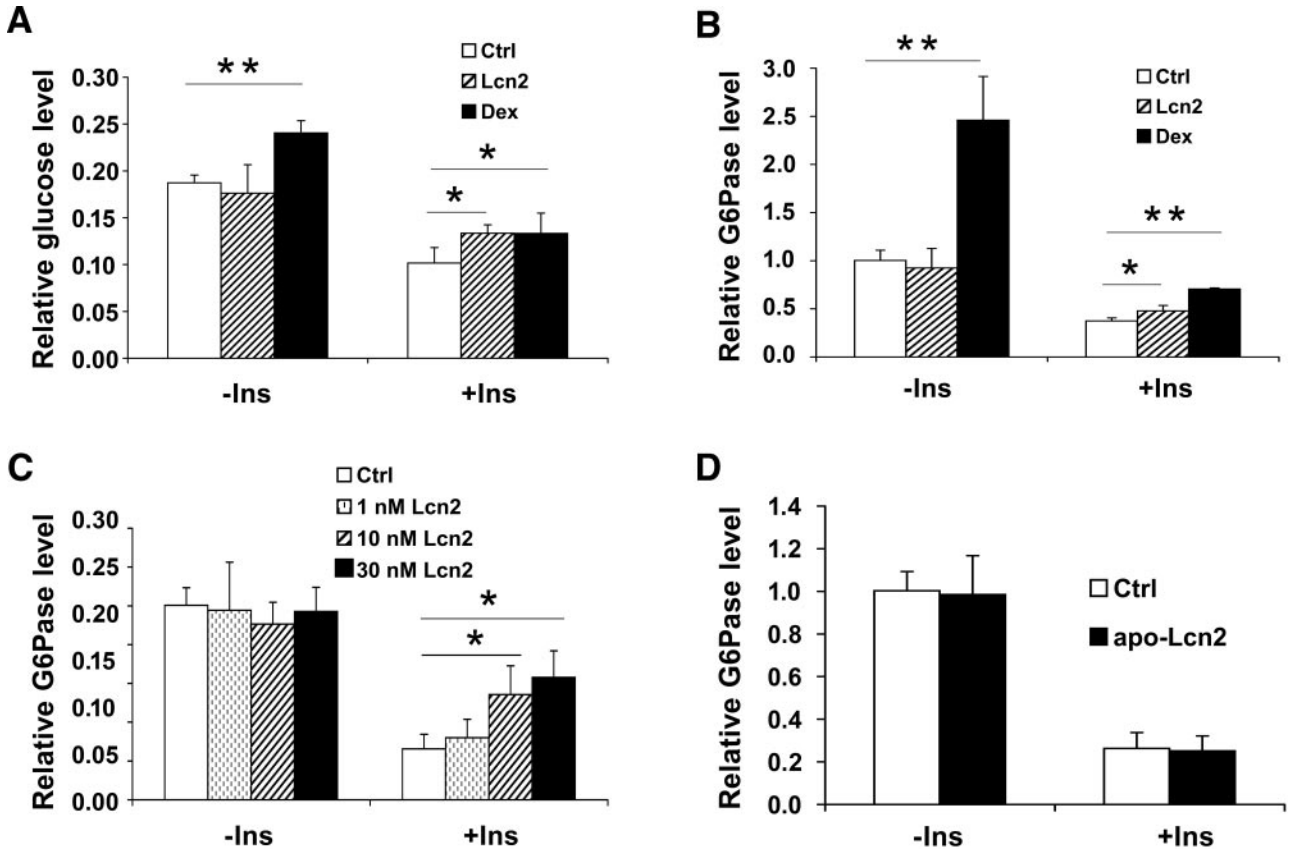

FIG. 6. Exogenous recombinant *Lcn2* induces insulin resistance in H4IIe hepatocytes. *A*, *left*: Glucose production induced by liganded *Lcn2* (10 nmol/l) or Dex (250 nmol/l) in the presence or absence of insulin (100 nmol/l). *A*, *right*: Effect of liganded *Lcn2* (10 nmol/l) or Dex (250 nmol/l) on glucose-6-phosphatase mRNA expression in the presence or absence of insulin (100 nmol/l). *B*: Dose response of liganded *Lcn2* on glucose-6-phosphatase expression. *C*: Effect of apo-*Lcn2* on glucose-6-phosphatase expression. Data are means ± SD, *$P < 0.05$, **$P < 0.01$, $n = 3$.

noted adipose expression of Lcn2 (16–19), our data are the first to demonstrate that adipocytes may be the dominant source of Lcn2 expression. Furthermore, we show that adipose-specific expression is dictated in large part by C/EBP-dependent *trans*-activation of a defined element in the *Lcn2* promoter. The lack of Lcn2 in brown adipose tissue is interesting and implies that WAT-specific factors besides C/EBP are required or that brown adipose tissue contains specific repressors of Lcn2 synthesis.

Lcn2 has been proposed to serve many functions, ranging from apoptosis to uterine involution to genitourinary development (12,22,23). Data obtained from knockout mice, however, suggest that Lcn2 serves as part of the innate immune system used as a nonspecific defense against microbes (10,11). In this capacity, Lcn2 expression occurs in inflamed epithelial tissues in direct contact with potential pathogens, such as respiratory and intestinal epithelium (24). Adipose tissue is not usually considered to be in direct contact with invading pathogens, but a large body of data has now accumulated suggesting that fat is intimately involved in immune activity and acute-phase response. Furthermore, obesity is considered to be a pro-inflammatory state with elevation of multiple markers of inflammation (25); increased Lcn2 seen in obese animals is consonant with this idea.

Based on the studies presented here, we propose that Lcn2 acts as an adipocyte-derived mediator of insulin resistance. This assertion is found on several lines of evidence, both direct and indirect. First, agents that promote insulin resistance induce the expression of Lcn2, including glucocorticoids and TNF-α. Similarly, hyperglycemia, which also reduces insulin sensitivity in adipocytes, causes enhanced expression of Lcn2 in adipocytes (26). Second, insulin-sensitizing thiazolidinedione compounds reduce the expression of Lcn2 in adipocytes (Fig. 4) (27). Third, Lcn2 is elevated in multiple murine models of obesity. Finally, reduction of Lcn2 in cultured adipocytes improved insulin sensitivity, demonstrating a direct link between this secreted molecule and cellular glucose homeostasis. The fact that exogenous Lcn2 did not affect glucose uptake in 3T3-L1 adipocytes (data not shown) is interesting and suggests that Lcn2 levels in media conditioned by the cultured adipocytes are already so high that adding more has no incremental effect. Interestingly, data from *db/db* mice (16,27) indicate that Lcn2 expression is elevated in the liver in this obese model; our data suggest that liver Lcn2 expression trends lower in high-fat–fed mice (data not shown). Thus, the contribution of extra-adipose sources of Lcn2 to serum is unclear and may differ between obesity models.

How might Lcn2 act to induce insulin resistance? Lcn2 has been proposed to be an iron delivery protein (22), and there is a well-known association between iron accumulation and diabetes (28). Patients with hemochromatosis, for example, have insulin resistance in addition to reduced insulin secretory capacity (28), and iron intake in healthy women has been positively associated with the risk of developing type 2 diabetes (29). Most of this effect has been inferred to involve hepatic insulin sensitivity (28); iron-mediated dysregulation of insulin action in adipocytes has never been explicitly assessed. Adipocytes certainly express iron-regulatory proteins, however, and iron has

been shown to mediate lipolysis in cultured fat cells (30). Consistent with the idea that iron is required for the effect of Lcn2 on insulin action, apo-Lcn2 was ineffective in causing insulin resistance in cultured hepatocytes. Iron may induce insulin resistance through the formation of specific reactive oxygen species, given the well-studied role of transition metals in catalyzing the Fenton reaction in cells. We have shown that reactive oxygen species act causally in multiple forms of insulin resistance in mice and in cultured adipocytes (15).

Lcn2 may also signal through a specific receptor, which may or may not involve the subsequent delivery of iron. Green and colleagues (31) cloned an organic cation transporter that is suggested to mediate Lcn2 internalization and downstream functions in multiple cell types. We have confirmed the expression of this molecule in brain and liver using Northern analysis and PCR but do not detect it in adipose tissue from mice or in 3T3-L1 cells at any stage of development (data not shown). This indicates that Lcn2 may exert its effects in adipocytes via another mechanism.

A recent study found that serum LCN2 levels are increased in obese humans, with excellent correlation between LCN2 and measures of insulin resistance in this population (27). We have seen that cytokines induce LCN2 expression in human subcutaneous adipocytes in a manner similar to that seen in 3T3-L1 cells (data not shown). These data suggest a possible role for LCN2 in human insulin resistance.

Our data suggest that Lcn2 may be added to the growing list of secreted molecules that adipocytes use to modulate glucose homeostasis. We are now testing this hypothesis directly in vivo in mice using both gain-of-function and loss-of-function approaches.

ACKNOWLEDGMENTS

This work was supported by National Institutes of Health Grants DK63906 (to E.D.R.) and DK43051 (to B.B.K.), and funding was provided by Takeda Pharmaceutical Co., Ltd.

Part of this study was presented as a poster at the 88th annual meeting of the Endocrine Society, Boston, Massachusetts, 24–28 June 2006.

We thank members of the Rosen and Kahn labs for helpful discussions. We extend a special thanks to Tonya Martin and Chris Wasson for technical help. We also thank Kiyoshi Mori and Jonathan Barasch for the gift of recombinant *Lcn2* and Karen Inouye for providing fractionated adipose samples.

REFERENCES

1. Kahn BB, Flier JS: Obesity and insulin resistance. *J Clin Invest* 106:473–481, 2000
2. Halaas JL, Gajiwala KS, Maffei M, Cohen SL, Chait BT, Rabinowitz D, Lallone RL, Burley SK, Friedman JM: Weight-reducing effects of the plasma protein encoded by the obese gene. *Science* 269:543–546, 1995
3. Rosen ED, Spiegelman BM: Adipocytes as regulators of energy balance and glucose homeostasis. *Nature* 444:847–853, 2006
4. Scherer PE, Williams S, Fogliano M, Baldini G, Lodish HF: A novel serum protein similar to C1q, produced exclusively in adipocytes. *J Biol Chem* 270:26746–26749, 1995
5. Fukuhara A, Matsuda M, Nishizawa M, Segawa K, Tanaka M, Kishimoto K, Matsuki Y, Murakami M, Ichisaka T, Murakami H, Watanabe E, Takagi T, Akiyoshi M, Ohtsubo T, Kihara S, Yamashita S, Makishima M, Funahashi T, Yamanaka S, Hiramatsu R, Matsuzawa Y, Shimomura I: Visfatin: a protein secreted by visceral fat that mimics the effects of insulin. *Science* 307:426–430, 2005
6. Steppan CM, Bailey ST, Bhat S, Brown EJ, Banerjee RR, Wright CM, Patel HR, Ahima RS, Lazar MA: The hormone resistin links obesity to diabetes. *Nature* 409:307–312, 2001
7. Yang Q, Graham TE, Mody N, Preitner F, Peroni OD, Zabolotny JM, Kotani K, Quadro L, Kahn BB: Serum retinol binding protein 4 contributes to insulin resistance in obesity and type 2 diabetes. *Nature* 436:356–362, 2005
8. Flower DR: The lipocalin protein family: structure and function. *Biochem J* 318:1–14, 1996
9. Goetz DH, Holmes MA, Borregaard N, Bluhm ME, Raymond KN, Strong RK: The neutrophil lipocalin NGAL is a bacteriostatic agent that interferes with siderophore-mediated iron acquisition. *Mol Cell* 10:1033–1043, 2002
10. Berger T, Togawa A, Duncan GS, Elia AJ, You-Ten A, Wakeham A, Fong HE, Cheung CC, Mak TW: Lipocalin 2-deficient mice exhibit increased sensitivity to Escherichia coli infection but not to ischemia-reperfusion injury. *Proc Natl Acad Sci U S A* 103:1834–1839, 2006
11. Flo TH, Smith KD, Sato S, Rodriguez DJ, Holmes MA, Strong RK, Akira S, Aderem A: Lipocalin 2 mediates an innate immune response to bacterial infection by sequestrating iron. *Nature* 432:917–921, 2004
12. Devireddy LR, Teodoro JG, Richard FA, Green MR: Induction of apoptosis by a secreted lipocalin that is transcriptionally regulated by IL-3 deprivation. *Science* 293:829–834, 2001
13. Mori K, Lee HT, Rapoport D, Drexler IR, Foster K, Yang J, Schmidt-Ott KM, Chen X, Li JY, Weiss S, Mishra J, Cheema FH, Markowitz G, Suganami T, Sawai K, Mukoyama M, Kunis C, D'Agati V, Devarajan P, Barasch J: Endocytic delivery of lipocalin-siderophore-iron complex rescues the kidney from ischemia-reperfusion injury. *J Clin Invest* 115:610–621, 2005
14. Rosen ED, Hsu CH, Wang X, Sakai S, Freeman MW, Gonzalez FJ, Spiegelman BM: C/EBPalpha induces adipogenesis through PPARgamma: a unified pathway. *Genes Dev* 16:22–26, 2002
15. Houstis N, Rosen ED, Lander ES: Reactive oxygen species have a causal role in multiple forms of insulin resistance. *Nature* 440:944–948, 2006
16. Lin Y, Rajala MW, Berger JP, Moller DE, Barzilai N, Scherer PE: Hyperglycemia-induced production of acute phase reactants in adipose tissue. *J Biol Chem* 276:42077–42083, 2001
17. Soukas A, Cohen P, Socci ND, Friedman JM: Leptin-specific patterns of gene expression in white adipose tissue. *Genes Dev* 14:963–980, 2000
18. Baudry A, Yang ZZ, Hemmings BA: PKBalpha is required for adipose differentiation of mouse embryonic fibroblasts. *J Cell Sci* 119:889–897, 2006
19. Kratchmarova I, Kalume DE, Blagoev B, Scherer PE, Podtelejnikov AV, Molina H, Bickel PE, Andersen JS, Fernandez MM, Bunkenborg J, Roepstorff P, Kristiansen K, Lodish HF, Mann M, Pandey A: A proteomic approach for identification of secreted proteins during the differentiation of 3T3-L1 preadipocytes to adipocytes. *Mol Cell Proteomics* 1:213–222, 2002
20. Friedl A, Stoesz SP, Buckley P, Gould MN: Neutrophil gelatinase-associated lipocalin in normal and neoplastic human tissues: cell type-specific pattern of expression. *Histochem J* 31:433–441, 1999
21. Rosen ED, MacDougald OA: Adipocyte differentiation from the inside out. *Nat Rev Mol Cell Biol* 7:885–896, 2006
22. Yang J, Goetz D, Li JY, Wang W, Mori K, Setlik D, Du T, Erdjument-Bromage H, Tempst P, Strong R, Barasch J: An iron delivery pathway mediated by a lipocalin. *Mol Cell* 10:1045–1056, 2002
23. Ryon J, Bendickson L, Nilsen-Hamilton M: High expression in involuting reproductive tissues of uterocalin/24p3, a lipocalin and acute phase protein. *Biochem J* 367:271–277, 2002
24. Cowland JB, Borregaard N: Molecular characterization and pattern of tissue expression of the gene for neutrophil gelatinase-associated lipocalin from humans. *Genomics* 45:17–23, 1997
25. Hotamisligil GS: Inflammation and metabolic disorders. *Nature* 444:860–867, 2006
26. Lin Y, Berg AH, Iyengar P, Lam TK, Giacca A, Combs TP, Rajala MW, Du X, Rollman B, Li W, Hawkins M, Barzilai N, Rhodes CJ, Fantus IG, Brownlee M, Scherer PE: The hyperglycemia-induced inflammatory response in adipocytes: the role of reactive oxygen species. *J Biol Chem* 280:4617–4626, 2005
27. Wang Y, Lam KS, Kraegen EW, Sweeney G, Zhang J, Tso AW, Chow WS, Wat NM, Xu JY, Hoo RL, Xu A: Lipocalin-2 is an inflammatory marker closely associated with obesity, insulin resistance, and hyperglycemia in humans. *Clin Chem* 53:34–41, 2007
28. Fernandez-Real JM, Lopez-Bermejo A, Ricart W: Cross-talk between iron metabolism and diabetes. *Diabetes* 51:2348–2354, 2002
29. Rajpathak S, Ma J, Manson J, Willett WC, Hu FB: Iron intake and the risk of type 2 diabetes in women: a prospective cohort study. *Diabetes Care* 29:1370–1376, 2006
30. Rumberger JM, Peters T Jr, Burrington C, Green A: Transferrin and iron contribute to the lipolytic effect of serum in isolated adipocytes. *Diabetes* 53:2535–2541, 2004
31. Devireddy LR, Gazin C, Zhu X, Green MR: A cell-surface receptor for lipocalin 24p3 selectively mediates apoptosis and iron uptake. *Cell* 123:1293–1305, 2005